

medRxiv preprint doi: <https://doi.org/10.1101/2020.05.16.20102947>; this version posted May 20, 2020. The copyright holder for this preprint (which was not certified by peer review) is the author/funder, who has granted medRxiv a license to display the preprint in perpetuity. It is made available under a CC-BY-ND 4.0 International license.

1 **Performance of progressive and adaptive COVID-19 exit strategies: a**
2 **stress test analysis for managing intensive care unit rates**

3

4 (10)(2e), (10)(2e), (10)(2e), (10)(2e),

5 (10)(2e) (2e), (10)(2e), (10)(2e), (10)(2e)

6 (10)(2e), (10)(2e), (10)(2e), (10)(2e)

7

8 ¹TNO, Netherlands Organization for Applied Scientific Research, The Hague, the
9 Netherlands.

10 ²Department of Pediatric Infectious Diseases and Immunology, Amsterdam Infection &
11 Immunity Institute, Amsterdam University Medical Centers, Emma Children's Hospital,
12 Amsterdam, the Netherlands.

13 ³Department of Intensive Care Medicine, Leiden University Medical Center, Leiden, the
14 Netherlands.

15 ⁴Department of Clinical Epidemiology, Biostatistics and Bioinformatics, Amsterdam Public
16 Health, Amsterdam University Medical Centers, University of Amsterdam, Amsterdam, the
17 Netherlands.

18 ⁵Faculty of Medicine, VUmc School of Medical Sciences, VU Amsterdam, Amsterdam, the
19 Netherlands.

20

21 *Correspondence to: (10)(2e) [@amsterdamumc.nl](mailto:(10)(2e)@amsterdamumc.nl)

22

23 **One Sentence Summary:** Progressive and adaptive COVID-19 exit strategies

24 **ABSTRACT**

25 **Background:** In May 2020, many European countries have begun to introduce an exit
26 strategy for the coronavirus disease 2019 (COVID-19) pandemic which involves relaxing
27 social distancing measures. Predictive epidemiological modeling indicates that chances for
28 resurgence are high. However, parametrization of the epidemiological nature of COVID-19
29 and the effect of relaxing social distancing is not well constrained, resulting in highly
30 uncertain outcomes in view of managing future intensive care unit (ICU) needs.

31 **Methods and findings:** For performance analysis of exit strategies we developed an
32 open-source ensemble-based Susceptible-Exposed-Infectious-Removed (SEIR) model. It takes
33 into account uncertainties for the COVID-19 parametrization and social distancing measures.
34 The model is calibrated to data of the outbreak and lockdown phase. For the exit phase, the
35 model includes the capability to activate an emergency brake, reinstating lockdown
36 conditions. Alternatively, the model uses an adaptive COVID-19 cruise control (ACCC)
37 capable to retain a targeted ICU level. The model is demonstrated for the Netherlands and we
38 analyzed progressive and adaptive exit strategies through a stress test of managing ICU rates.
39 The progressive strategy reflects the outcome of social and economic pressure to use one-way
40 steering toward progressively relaxing measures at an early stage. It is marked by a high
41 probability for the activation of the emergency brake due to an unsolicited growth of ICU
42 needs in the following months. Alternatively, the two-way steering ACCC can flatten ICU
43 needs in a more gradual way and avoids activation of the emergency brake. It also performs
44 well for seasonal variation in the reproduction number of severe acute respiratory syndrome-
45 coronavirus.

46 **Conclusions:** The adaptive strategy (ACCC) is favored, as it avoids the use of the
47 emergency brake at the expense of small steps of restrictive measures and allows the
48 exploration of riskier and potentially rewarding measures in the future pathways of the exit
49 strategy.

medRxiv preprint doi: <https://doi.org/10.1101/2020.05.16.20102947>; this version posted May 20, 2020. The copyright holder for this preprint (which was not certified by peer review) is the author/funder, who has granted medRxiv a license to display the preprint in perpetuity. It is made available under a [CC-BY-ND 4.0 International license](#).

- 50 **Performance of progressive and adaptive COVID-19 exit strategies: a**
51 **stress test analysis for managing intensive care unit rates**
52
53 Jan-Diederik van Wees, Martijn van der Kuip, Sander Osinga, David van Westerloo, 
54 Tanck, Maurice Hanegraaf, Maarten Pluymaekers, Olwijn Leeuwenburgh, Lonneke van
55 Bijsterveldt, Pien Verreijdt, Logan Brunner, Marceline Tutu van Furth

56 INTRODUCTION

57 According to the World Health Organization (WHO), coronavirus disease 2019
58 (COVID-19) reached the pandemic phase on 11 March 2020 (1). On 15 May 2020, the severe
59 acute respiratory syndrome-coronavirus (SARS-CoV-2) virus had spread to 213 countries
60 worldwide, leading to 4,586,270 registered infections and 306,063 deceased (2). To control
61 COVID-19, various measures have been undertaken ranging from liberal control in Sweden
62 and test and quarantine policies in South Korea, to complete prolonged lockdowns in Italy
63 and Spain (3). The chosen measures of national policymakers are based on testing capacity,
64 characteristics of specific societies and more importantly on the phase of the outbreak:
65 containment, suppression or mitigation (4). 'All countries must strike a fine balance between
66 protecting health, preventing economic and social disruption, and respecting human rights'
67 (1). In the Netherlands, a targeted lockdown based on social distancing, was introduced on 16
68 March 2020 (5).

69 As the trend of death rates (Fig. 1) and hospital admissions are slowly showing a
70 flattening curve and intensive care units (ICU) no longer work at or above their capacity,
71 many countries have begun to introduce an exit strategy which involves relaxing social
72 distancing measures. Predictive epidemiological modeling demonstrated that prolonged
73 and/or intermittent periods of social distancing are required to mitigate the possibility of
74 resurgences of infection (6, 7). They have not been calibrated to (near) real-time data and did
75 not consider quantitative measurement and control systems to assess and mitigate unsolicited
76 stress to the health care system. Moreover, these models highlight that parametrization of the
77 epidemiological nature of COVID-19 is not well constrained and highly uncertain (4, 6-8). For
78 this reason, models may be perceived as unreliable in light of all the uncertainties considered,
79 and in turn the lack of reliable models causes a major challenge in robustly designing and
80 testing exit strategies.

81 In order to cope with large uncertainties for correct parametrization of transmission
82 models and the effect of social distancing measures, we propose a data-driven and holistic
83 approach for calibrating transmission models and the effects of non-pharmaceutical
84 interventions under large uncertainty. To this end, we used a fast, ensemble based
85 Susceptible-Exposed-Infectious-Removed (SEIR) meta-population model explained in
86 methods, which can be calibrated daily to observed data. As a starting point for the exit
87 strategy, the model uses the posterior ensembles and the underlying model and intervention
88 parameters, which have been calibrated to data of the outbreak and lockdown phase (Fig. 2).
89 This provides a robust model basis for a (real-time) analysis and stress test of appropriate exit
90 strategies, and underlying uncertainty. Furthermore, since the model is open-source and can
91 build from public data sources and is not dependent on detailed epidemiological field study
92 results, such as testing or contact-tracing information, it can contribute to the need of the
93 scientific community for accelerated development of open modeling approaches to study exit
94 strategies (9).

95 Two ‘safe’ exit strategies as outlined in Fig. 2 have been put to a stress test in a case
96 study for the Netherlands. Both aim at maximizing the positive effect on social distancing and
97 reducing risks for the healthcare system at the same time. They consider (step-changed)
98 relaxation in conjunction with possible restrictive measures, in view of managing the risk for
99 exceeding threshold levels for ICU capacity. The two strategies differ fundamentally in ICU
100 objectives and approach. The progressively relaxing and ‘emergency brake’ strategy reflects
101 the outcome of social and economic pressure to use one-way steering toward progressively
102 relaxing and rather early steps and it is marked by a high probability for the need of the use
103 of an emergency brake due to an unsolicited growth of ICU needs in the following months.
104 Alternatively, the Adaptive COVID-19 Cruise Control (ACCC) is based on two-way steering
105 and can flatten ICU needs in a more gradual way to a given nominal capacity. We will show
106 that the ACCC strategy can avoid the need for an emergency brake, and also performs well if

107 the potential effect of seasonal variation in the reproduction number of SARS-CoV-2 is taken
108 into account (7).

109

110 METHODS

111 For the modeling, we used an ensemble-based SEIR metapopulation model to simulate
112 the epidemics (8, 10), which incorporates the effect of measures to reduce community
113 spreading (4, 8). The model is largely based on van Wees et al., 2020 (11), and has been
114 expanded in this study to incorporate a more realistic flow process for hospitalization and
115 ICU (Fig. 3).

116 The SEIR model stands for the following: Susceptible: the susceptible part of the
117 population; Exposed: the part of the population that carries the virus; Infected: patients
118 showing the first mild symptoms; Removed: patients that have recovered or died.
119 Mathematically, the SEIR compartments are modeled as fractions of the population, initially
120 susceptible to the virus. Subsequently, we solve the following differential equations starting
121 from initial values for $S = 1 - 1/N$, $E = 1/N$ and setting I and R to 0. N is ratio of population size
122 and exposed persons introduced at the start of the simulation. The initial day of introduction
123 of the virus is 15 days prior to the first registered case, and the density of the virus per N is
124 varied to obtain a first order fit with the observed number of registered infections,
125 hospitalized, death. The differential model is formulated as follows:

$$126 \quad S' = -(1 - \alpha(t))\beta(t)SI$$

$$127 \quad E' = (1 - \alpha(t))\beta(t)SI - \sigma E$$

$$128 \quad I' = \sigma E - \gamma I$$

$$129 \quad R' = \gamma I$$

130 The R compartment is extended with the flow scheme for the hospitalization and ICU
131 treatment process as depicted in Fig. 3. For the incorporation of the logistic spread of patients,
132 the model adopts successive convolutions of the R prediction, with a Gamma distribution for

133 delay, recovery and treatment times d_{nosr} , d_{nosrec} , d_{nosdr} , d_{icurec} and d_{icud} (Fig. 3, Table 1). The
 134 simulation incorporates the strength of social distancing through the parameter $\alpha(t)$: $\alpha(t)$ is 0
 135 when no measures are in place and 1 when social distancing would prevent any transmission
 136 (8). The ensemble-based workflow intrinsically allows for the use of large uncertainties
 137 underlying the relaxing and restrictive steps in social distancing and can therefore be used
 138 effectively for stress tests of exit scenarios. Our model is strongly data-driven and calibrates
 139 prior estimates for a number of model parameters (Table 1), including the reproduction
 140 number, strength of social distancing, and some of the treatment times for hospitalization and
 141 ICU from the observed data. For data assimilation of all parameters in conjunction with
 142 calibration of $\alpha(t)$, we use the ensemble smoother with multiple iterations which is a
 143 computationally efficient method for ensembles of non-linear forward models (12). The data
 144 assimilation is performed by matching modeled hospitalization and ICU usage to reported
 145 usage. We adopted ensembles of 500 realizations and a value of 70 and 20 for the error in
 146 standard deviation in reported bed count for hospitalization and ICU, respectively.

147 Once the model has been calibrated to the data of the outbreak and lockdown phase,
 148 in the exit strategies the relaxing or restrictive measures for social distancing are adopted by
 149 a step-wise change of the posterior $\alpha(t)$ values, such that $\alpha(t > t_{step}) = \alpha(t) + \Delta\alpha(t)$ at given times
 150 or at specific time intervals t_{step} . In the model, $\Delta\alpha(t) = N(m_{step}, s_{step})$ of each step is normally
 151 distributed with m_{step} = mean and s_{step} = standard deviation. For each member in the ensemble,
 152 a sample is taken for $\Delta\alpha(t)$. Based on the updated $\alpha(t)$, the model is rerun. The resulting ICU
 153 occupancy is monitored daily in the model. If the ICU occupancy or the ICU growth rate
 154 exceeds a given level, the emergency brake is activated. The emergency brake reinstates
 155 lockdown conditions by adopting $\alpha(t > t_{emergencybrake}) = N(m_{lockdown}, s_{lockdown})$, where $m_{lockdown}$ and
 156 $s_{lockdown}$ are based on the posterior distribution of $\alpha(t)$ in the data calibration of the lockdown
 157 phase. In the aftermath of the emergency brake, the renewed lockdown conditions can be
 158 followed by renewed steps for relaxation of social distancing, once the resulting ICU

159 occupancy drops to acceptable levels. In the progressive exit strategy only user-defined
160 relaxing measures ($m_{step}<0$) are considered for social distancing.

161 In the adaptive exit strategy, we consider the ACCC to automatically steer both
162 relaxing ($m_{step}<0$) and restrictive step-changes ($m_{step}>0$) toward reaching and retaining a
163 sustainable level of nominal ICU capacity and to avoid activation of the emergency brake and
164 renewed lockdown conditions. To this end, the need for a step-change and its sign is
165 monitored at intervals of two weeks, taking the actual ICU occupancy, ICU growth rate and
166 change in growth rate of the past two weeks of the ensemble member, and then using an
167 extrapolated value from a second-order Taylor approximation that looks one week ahead. If
168 the extrapolated growth rate (and value) is moving away from the targeted nominal capacity,
169 a relaxing (when below target) or restrictive (when above target) step is adopted. A
170 constrictive step is taken if the change in growth rate is accelerating toward the target. For the
171 time following the first relaxation steps after the lock down, this effectively means that steps
172 are taken to slow down the growth rate as soon as the look ahead signals a rise in ICU
173 occupancy.

174

175 RESULTS

176 *The Netherlands' outbreak and lockdown phase*

177 With a population density of $\sim 1,300/\text{mi}^2$, the Netherlands (~ 17.1 million citizens)
178 ranks number 32 worldwide in population density (in perspective New York state: ~ 19.5
179 million citizens and $\sim 420/\text{mi}^2$ and USA overall density of $\sim 95/\text{mi}^2$) (13). In the era before
180 COVID-19, the ICU capacity was 1,150 and occupied for $\sim 75\%$. In the Netherlands, the first
181 patient with COVID-19 was diagnosed on 27 February 2020. At the peak of the outbreak on 2
182 April 2020, 1,332 patients with COVID-19 were admitted at an ICU. The current maximum
183 national capacity is 1,800 ICU including non-COVID-19 care (14) In the remainder of this
184 paper we refer to COVID-19 ICU capacity only.

185 The daily admittance of ICU patients closely followed the trend of hospitalized
186 patients (Fig. 4). Markedly, the fraction of hospitalized patients that required an ICU shows a
187 gradual decreasing trend toward a relatively constant of 20% from the end of March onwards.
188 The case fatality of ICU patients is 30% (14) and the overall mortality of COVID-19 patients
189 (5,643 on 14 May 2020) in the Netherlands contributes to ~2% of the global death toll of the
190 pandemic (Fig. 1) (2). The cumulative ICU mortality is approximately 10% of the registered
191 COVID-19 death toll in the Netherlands. This can be well explained by the fact that
192 approximately 80% of ICU patients are below the age of 70 (14), whereas 90% of the total
193 mortality is in the age groups of 70 and older (15). Also, hospitalized patients are skewed
194 toward younger patients, with approximately 50% below the age of 70 (16). These numbers
195 highlight that hospital and ICU admittance in the Netherlands is directed towards younger
196 age groups compared to earlier studies assessing hospitalization and ICU needs (4). This
197 admittance practice significantly reduced pressure on the health care system.

198 The forecast presented here, has been based on the data until 30 April 2020, calibrating
199 the prior model parameters to the observed data on hospitalized and ICU patients, as well as
200 mortality prior to 7 April 2020. The forecast includes 500 ensemble members, and 8 iterations
201 were used in the ensemble smoother for the calibration to the data. The time-invariant prior
202 and resulting posterior model parameters are listed in Table 1. In the model prior $\alpha(t)$ values,
203 have been chosen based on expert judgement and are in the range of values used in literature
204 (8), based on the logic of contact reduction and social distancing (4, 8). They have been
205 introduced on the dates of government measures (11), with a time-interval of 5-10 days and
206 adopted a relatively large a-priori uncertainty for the social distancing strength $\alpha(t)$ with a
207 standard deviation of 10-30% of its estimated value (11). The posterior time-variant strength
208 of the effect of social distancing, reducing the transmission strength by $1-\alpha(t)$, and the
209 predicted model results for infected, hospitalized and ICU patients and mortality are shown
210 in Fig. 5A-E. The social distancing strength (Fig. 5A) have been adjusted in the ensemble

211 smoother to fit data on hospitalized (Fig. 5C) and ICU occupancy (Fig. 5D). The model is very
212 well capable of reproducing the observed hospitalization (Fig. 5C) and ICU rates (Fig. 5D) and
213 demonstrates the effectiveness of the social distancing in terms of reducing the hospitalization
214 inflow, resulting in a peak ICU occupancy in early April 2020 followed by a downward trend
215 to manageable levels on 30 April 2020 close to an occupancy of 700 ICU patients. It is expected
216 that ICU usage will further reduce well below 600 on 11 May 2020, the date the Dutch
217 government has been planning to relax the lockdown conditions. The posterior $1-\alpha(t)$
218 evolution is marked by a rapid stepwise decrease in March 2020, in line with the government
219 restrictions. The confidence bandwidth of the $1-\alpha(t)$ values shown in Fig. 5A is consistent with
220 the data and the prior model parameter uncertainty and possible combinations in temporal
221 change of $\alpha(t)$ resulting from data assimilation process. After 7 April 2020 in the model, the
222 $\alpha(t)$ has been considered invariable through time, resulting in a relatively narrow bandwidth
223 of future forecasts for ICU needs.

224 The mortality beyond 7 April 2020 is significantly higher than expected from the
225 hospitalization flow model. One possible explanation for this strong deviation, is that a
226 growing share of the registered deceased patients are related to care centers dedicated to
227 elderly people (Fig. 5E). Here COVID-19 has been marked by more active spreading than the
228 national trend in the last three weeks of April 2020. This may be related to a lack of testing
229 and protective measures for care-giving personnel in that setting of elderly care. It should also
230 be noted that overall many more casualties are related to COVID-19 than tested. It is estimated
231 from nationally recorded death rates that the real death toll of COVID-19 may be twice as high
232 as the registered rates indicate (15). The same applies to estimates of the fraction of the Dutch
233 population which may have been infected. Based on blood samples from Sanquin, the Dutch
234 national blood bank, up to 3.6% of the Dutch population may have been infected since the
235 outbreak (17). For this reason, we assumed in the prior of the model prior parameters that a
236 relatively low fraction (1.5%) of those infected people gets hospitalized. Consequently, the

237 predicted number of cumulative infected is significantly higher in the model than actual
238 confirmed cases (Fig. 5B). The SEIR model takes into account the effects of gradual build-up
239 of immunity through the gradual reduction of S in the mathematical formula (see methods).
240 Such a reduction can potentially contribute to social relaxation and therefore the estimation
241 of the ratio of infected and hospitalized patients is important. However, with the adopted
242 parameters, the effect of immunity build-up is rather low and not of significant influence for
243 the presented results in this paper.

244

245 *Progressively relaxing exit strategy with emergency brake*

246 For the progressively relaxing strategy we considered six scenarios (Fig. 6A-F), in
247 order to highlight key aspects of this approach and the effects of the emergency brake. The
248 first scenario is marked by a relatively large step-change, reducing on 11 May 2020 the social
249 distancing strength $\alpha(t)$ from approximately 0.8 to 0.6 with $\Delta\alpha(t) = N(-0.2, 0.05)$. In absence of
250 renewed mitigation measures, the ICU needs would grow unboundedly within a couple of
251 months as displayed in Fig. 6A.

252 In the second scenario (Fig. 6B), the first scenario is complemented with an emergency
253 brake. This emergency brake is triggered either by reaching 700 ICU occupancy or if the daily
254 growth rate in ICU occupancy exceeds 20 (depicted with the colored dots in the right panels
255 of Fig. 6). The underlying full ensemble results of this scenario are also shown in Fig. 7 to
256 highlight the functioning of the emergency brake. The brake reinstates the proven social
257 distancing measure of the lockdown phase with $\alpha(t) = N(0.8, 0.05)$. Effectively, this results in
258 peak ICU values which can reach up to 700-1,400 admissions. Most of the peak values in the
259 ensemble are in the range of 800-1,000 ICU beds, highlighting the long delay between the
260 activation of the brake and its effect in the ICU occupancy. Due to this delay the peak ICU
261 value is expected to show a correlation with the growth rate of ICU occupancy at the time the

262 emergency brake was activated. This can indeed be observed in the ensemble results in Fig.
263 7.

264 In the third scenario (Fig. 6C), the step-change exit strategy adopts the relaxation in
265 five smaller step-changes with $\Delta\alpha(t) = N(-0.04, 0.01)$, in intervals of three weeks' time, instead
266 of a single step-change of -0.2. The gradual relaxation results in a more gradual increase in
267 daily ICU needs for the entire ensemble when compared to the single step-change.
268 Consequently, the emergency brake results in a lower peak of ICU admissions, marked by
269 most of the predicted peak values between 700 and 900, and no outliers higher than 1,000.

270 In the fourth scenario (Fig. 6D), we extend the third scenario with taking progressively
271 relaxing social distancing steps in the aftermath of the emergency brake. The initiation of
272 renewed progressive steps follows after the ICU drops below 500. The relaxing steps can in
273 turn reactivate the emergency brake and consequently a cyclic pattern occurs.

274 In the fifth scenario (Fig. 6E), we extend the previous scenario with seasonal variation
275 in the reproduction number of SARS-CoV-2 (7) and evaluate its effect on waxing and waning
276 of social relaxation. For the seasonal variation, we adopt a maximum R_0 at the start of the
277 model on 1 March 2020 ($R_0 \sim 3.4$), and a minimum at 70% on 1 September 2020 ($R_0 \sim 2.4$), varied
278 with a cosine function.

279 Finally, the last scenario (Fig. 6F) takes a more conservative, progressively relaxing
280 approach in which the number of relaxing steps is limited to 2, and on average $\alpha(t) > (1-1/R_0)$,
281 resulting in a continuous down trend in ICU. In this scenario the emergency brake is only
282 triggered at the start, in a very limited number of members of the posterior. In the remainder
283 of the two years after the two progressive steps no emergency brake is used.

284 In summary, for the progressively relaxing exit scenario, a large step-change results in
285 a relatively early and possibly high peak, whereas if the change is implemented in more
286 gradual, smaller step-changes, the peak in ICU admissions is delayed and lowered. In both
287 scenarios, the emergency brake is capable of limiting forecasted ICU peaks in bounds of the

288 1,800-peak capacity in the Netherlands, but any scenario of progressively relaxing steps is at
289 some point likely to result in acceleration of growth and the triggering of the emergency brake.
290 Therefore, progressive step-change scenarios inevitably result in a high probability of a
291 resurgence of infected cases, requiring the need for mitigation measures within the first
292 months up until the first year after the relaxing of social distancing. $1-\alpha(t)$ causes the daily
293 infections and hospitalized cases to rise. Such conditions can also be further amplified in case
294 unsolicited growth is caused by seasonal variation of the reproduction number (7).

295

296 *The adaptive COVID-19 cruise control exit strategy*

297 As an alternative to the progressively relaxing exit strategy, we consider the ACCC to
298 steer the step-changes toward reaching and retaining a sustainable level of nominal ICU
299 capacity. For the ACCC's target ICU nominal capacity, we consider two scenarios: 200 and
300 400 ICU patients, respectively. We adopt step changes of the same size as the progressive exit
301 strategy $\Delta\alpha(t) = N(\pm 0.04, 0.01)$. Other settings are the same as in the previous scenarios, except
302 for the emergency brake for the high scenario, where the emergency threshold level for ICU
303 and daily ICU growth have been raised to 1,400 and 40, respectively. The ACCC (Fig. 8A and
304 8B) is well capable in steering toward the ICU nominal target levels without activating the
305 emergency brake. The gain in relaxation of social distancing in the high scenario is limited,
306 resulting in $\alpha(t)$ which on average is only a fraction lower (~ 0.03) than the low scenario, but
307 grows to ~ 0.05 in the last year due to slightly faster build-up of group immunity. From the
308 minor gain in social relaxation, it could be argued that the low scenario should be favored,
309 considering the more positive health effects.

310 Within an alternative scenario, we consider seasonal variation in the reproduction as
311 for the progressive relaxation scenarios (conform Fig. 6E). The results are shown for a period
312 of two years in Fig. 8C and 8D, causes an appropriate adaptive response of the ACCC, marked
313 by significant seasonal variation in $\alpha(t)$, while maintaining target ICU levels.

314 In conclusion, the ACCC strategy can effectively steer toward the targeted nominal
315 ICU rates, and the adaptive capability allows it to closely follow seasonal variation in R_0 . In
316 both the low and high scenarios, the emergency brake is never activated proving ICU needs
317 remain below 700 and 1,400 ICU respectively at all times for all ensemble runs.

318

319 DISCUSSION

320 We analyzed two dissimilar ways to exit the lockdown that most countries worldwide
321 are enduring. A progressively relaxing strategy can initially lead to a significant reduction of
322 distancing measures but is likely related to a high peak resurgence of COVID-19 cases for
323 which inevitably an emergency brake will be needed. Alternatively, our ACCC approach
324 leads to small incremental, and constantly evaluated steps in reduction of restrictions and
325 restraining measures if necessary. The ACCC leads to a more gradual and sustainable release,
326 as it does not need to activate the emergency brake. For this reason, we prefer the ACCC
327 approach. Both strategies effectively restrict the number of ICU admissions, however both
328 also indicate that to restrict the number of ICU admissions during an exit strategy the level of
329 safe release of social distancing measures will unfortunately be rather small. In our case study
330 of the Netherlands, increasing total ICU capacity in the ACCC only minimally increases the
331 level of potential release of measures.

332 A key assumption in both strategies is that we can take limited and controlled step-
333 change sizes. However, in practice, the uncertainty of the effect of each proposed step could
334 be very high. During the exit strategy, assessing and limiting the uncertainty of the effects of
335 each step change is critically important to be able to increase the reliability of prediction and
336 guide the steering of exit strategies. Many proposals for exit scenarios consider further
337 differentiation into age, social, and risk-prone groups, for example, adding to complexity and
338 uncertainty. Evidently, research into transmission characteristics considering different
339 measures can significantly help to reduce uncertainty. However, such an approach can be

340 slow and cumbersome, and will inevitably funnel the choice of controllable steps toward those
341 which are proven, can be tested and monitored and/or are marked by little uncertainty. This
342 can lead to restraints in embracing progressively relaxing steps with uncertain outcomes. The
343 ACCC approach can open pathways toward taking limited risks to empirically explore new
344 avenues in social distancing, since we can timely counteract negative outcomes of relaxing
345 steps with follow-up restrictive steps. The explorative approach can be further enhanced
346 through appropriate diversification of measures at risk, using financial methods such as
347 modern portfolio theory (18) and considering portfolios of uncorrelated measures (e.g. for
348 subpopulations, sectors, age groups, etc.). This will not only help reducing the intrinsic
349 uncertainty of step-changes to much lower values, but at the same time it can accelerate the
350 learning path of the effect of the many different measures considered. In addition, the ACCC
351 can be improved by replacing the rather simple look ahead function by more advanced
352 machine learning and ensemble-based forecasting techniques.

353 The presented ensemble-based, data-driven and holistic model workflow in this study
354 is fully open source and can promote analysis and further development of exit strategies in
355 other countries, with alternative demographic and transmission characteristics, different
356 social structures, hospital and ICU admittance practices, and a different history of outbreak
357 and lockdown management. Data needed are limited, requiring most importantly
358 hospitalization and ICU admittance, mortality and recovery numbers, and information on
359 past government measures. The emergency brake threshold levels for ICU occupancy and
360 daily ICU growth rate need to be adapted and are recommended to be approximately 40-70%
361 and 0.5-2% of maximum ICU capacity respectively, depending on available lockdown
362 measures and the considered exit strategy.

medRxiv preprint doi: <https://doi.org/10.1101/2020.05.16.20102947>; this version posted May 20, 2020. The copyright holder for this preprint (which was not certified by peer review) is the author/funder, who has granted medRxiv a license to display the preprint in perpetuity. It is made available under a [CC-BY-ND 4.0 International license](#).

363 **Acknowledgments:** We thank Anke Zindler for helpful comments.

364

365 **Funding:** none.

366

367 **Author contributions:** Conceptualization: J-D.v.W., S.O., M.P., O.L., L.v.B., L.B. Data curation:

368 J-D.v.W., S.O., M.P., O.L., L.v.B., L.B., M.T. Investigation: J-D.v.W., S.O., M.P., O.L., L.v.B., L.B.

369 Methodology: J-D.v.W., S.O., M.P., O.L., L.v.B., L.B. Visualization: J-D.v.W., M.v.d.K., P.V.

370 Software: J-D.v.W., S.O., M.P., O.L., L.v.B., L.B. Supervision: M.H. Writing, original draft: J-

371 D.v.W., M.v.d.K., M.T.v.F. Writing, review, and editing: all authors.

372

373 **Competing interests:** Authors declare no competing interests.

374

375 **Data and materials availability:** We collected the data from publicly available data sources

376 (2, 14, 16). The modeling code and data used for our analysis is available under (19).

medRxiv preprint doi: <https://doi.org/10.1101/2020.05.16.20102947>; this version posted May 20, 2020. The copyright holder for this preprint (which was not certified by peer review) is the author/funder, who has granted medRxiv a license to display the preprint in perpetuity. It is made available under a CC-BY-ND 4.0 International license.

377 **REFERENCES**

- 378 1. World Health Organization (WHO). "Coronavirus disease (COVID-19) situation report-
379 51" (2020); Available from: [https://www.who.int/docs/default-
380 source/coronaviruse/situation-reports/20200311-sitrep-51-covid-
381 19.pdf?sfvrsn=1ba62e57_10](https://www.who.int/docs/default-source/coronaviruse/situation-reports/20200311-sitrep-51-covid-19.pdf?sfvrsn=1ba62e57_10)
- 382 2. Worldometer. "COVID-19 coronavirus pandemic" (2020); Available from:
383 <https://www.worldometers.info/coronavirus/>
- 384 3. World Health Organization (WHO) regional office for Europe. "COVID-19 Health
385 system response monitor" (2020); Available from:
386 <https://www.covid19healthsystem.org/searchandcompare.aspx>
- 387 4. Imperial College COVID-19 Response Team. "Report 9: Impact of non-pharmaceutical
388 interventions (NPIs) to reduce COVID-19 mortality and healthcare demand" (2020);
389 Available from: [https://www.imperial.ac.uk/media/imperial-
390 college/medicine/sph/ide/gida-fellowships/Imperial-College-COVID19-NPI-
391 modelling-16-03-2020.pdf](https://www.imperial.ac.uk/media/imperial-college/medicine/sph/ide/gida-fellowships/Imperial-College-COVID19-NPI-modelling-16-03-2020.pdf)
- 392 5. Enserink M, Kupferschmidt K. With COVID-19, modeling takes on life and death
393 importance. *Science*. 2020;367(6485):1414-5.
- 394 6. Verity R, Okell LC, Dorigatti I, Winskill P, Whittaker C, Imai N, et al. Estimates of the
395 severity of coronavirus disease 2019: a model-based analysis. *Lancet Infect Dis*. 2020;pii:
396 S1473-3099(20)30243-7.
- 397 7. Kissler SM, Tedijanto C, Goldstein E, Grad YH, Lipsitch M. Projecting the transmission
398 dynamics of SARS-CoV-2 through the postpandemic period. *Science*. 2020;pii: eabb5793.
- 399 8. Lin Q, Zhao S, Gao D, Lou Y, Yang M, [\(10/20\)](#) SS, et al. A conceptual model for the
400 coronavirus disease 2019 (COVID-19) outbreak in Wuhan, China with individual
401 reaction and governmental action. *Int J Infect Dis*. 2020;93:211-6.

medRxiv preprint doi: <https://doi.org/10.1101/2020.05.16.20102947>; this version posted May 20, 2020. The copyright holder for this preprint (which was not certified by peer review) is the author/funder, who has granted medRxiv a license to display the preprint in perpetuity. It is made available under a CC-BY-ND 4.0 International license.

- 402 9. Barton CM, Alberti M, Ames D, Atkinson JA, Bales J, Burke E, et al. Call for
403 transparency of COVID-19 models. *Science*. 2020;368:482-3.
- 404 10. van Wees J-D, Osinga S, van der Kuip M, Tanck M, Hanegraaf M, Pluymaekers M, et al.
405 Forecasting hospitalization and ICU rates of the COVID-19 outbreak: an efficient SEIR
406 model.[Submitted]. E-pub: 30 March 2020.
407 doi:<http://dx.doi.org/10.2471/BLT.20.256743> *Bull World Health Organ*.
- 408 11. Wu JT, Leung K, Leung GM. Nowcasting and forecasting the potential domestic and
409 international spread of the 2019-nCoV outbreak originating in Wuhan, China: a
410 modelling study. *Lancet*. 2020;395:689-97.
- 411 12. Emerick AA, Reynolds AC. Ensemble Smoother With Multiple Data Assimilation.
412 *Computers & Geosciences*. 2013;55:3-15.
- 413 13. Worldpopulationreview. "Countries by density 2020"; Available from:
414 <https://worldpopulationreview.com/countries/countries-by-density/>
- 415 14. Stichting NICE. "COVID-19 infecties op de IC's [in Dutch]" (2020); Available from:
416 <https://www.stichting-nice.nl>
- 417 15. Rijksinstituut voor Volksgezondheid en Milieu (RIVM). "Monitoring sterftcijfers
418 Nederland", 4 May 2020"; Available from: <https://www.rivm.nl/monitoring-sterftcijfers-nederland>
- 419 [sterftcijfers-nederland](https://www.rivm.nl/monitoring-sterftcijfers-nederland)
- 420 16. Rijksinstituut voor Volksgezondheid en Milieu (RIVM). "Epidemiologische situatie
421 COVID-19 in Nederland 6 mei 2020"; Available from:
422 [https://www.rivm.nl/documenten/epidemiologische-situatie-covid-19-in-nederland-](https://www.rivm.nl/documenten/epidemiologische-situatie-covid-19-in-nederland-6-mei-2020)
423 [6-mei-2020](https://www.rivm.nl/documenten/epidemiologische-situatie-covid-19-in-nederland-6-mei-2020)
- 424 17. Rijksinstituut voor Volksgezondheid en Milieu (RIVM). "COVID-19 Technische briefing
425 Tweede Kamer, 22 april 2020 door [\(10\)20e](#) [\(10\)20e2](#) [\(10\)20e](#) [Technical briefing to parliament; 22
426 April 2020 by [\(10\)20e](#) [\(10\)20e2](#) [\(10\)20e](#)"]; Available from:

medRxiv preprint doi: <https://doi.org/10.1101/2020.05.16.20102947>; this version posted May 20, 2020. The copyright holder for this preprint (which was not certified by peer review) is the author/funder, who has granted medRxiv a license to display the preprint in perpetuity. It is made available under a CC-BY-ND 4.0 International license.

- 427 https://www.tweedekamer.nl/sites/default/files/atoms/files/20200422_techische_b
- 428 [riefing](#) (10)(2e) (10)(2e) (10)(2e) [rijvm_22_april.pdf](#)
- 429 18. Markowitz H. Portfolio Selection. The Journal of Finance. 1952;7:77-91.
- 430 19. Available from: <https://github.com/TNO/Covid-SEIR>
- 431

medRxiv preprint doi: <https://doi.org/10.1101/2020.05.16.20102947>; this version posted May 20, 2020. The copyright holder for this preprint (which was not certified by peer review) is the author/funder, who has granted medRxiv a license to display the preprint in perpetuity. It is made available under a CC-BY-ND 4.0 International license.

432 TABLE 1

433

Parameter	E_{mean}	E_{stddev}	G_{stddev}	Unit	Description
N	80,000 (65,840)	40,000 (17,691)	-	-	$1/N$ is the starting fraction of exposed in SEIR model
M	0.9	-	-	-	Fraction of total population susceptible to COVID-19 (16)
R_0	3.2 (3.4)	0.5 (0.1)	-	day ⁻¹	Initial reproduction number
σ	0.2	-	-	day ⁻¹	Incubation time of 5 days (10)
γ	0.5	-	-	day ⁻¹	Removal rate of infected people in self quarantine
d_{hos}	7	-	2	days	Days of illness before hospitalization
d_{hosd}	3	1	2	days	Days of hospital treatment for mortalities
d_{hosrec}	9	-	4	days	Days of hospital treatment for recovery
d_{icud}	11	-	8	days	Days of ICU treatment for mortalities (estimated from data fit Fig. 4)
d_{icurec}	24 (25)	1 (0.3)	19	days	Days of ICU treatment for recoverable case (estimated from data fit Fig. 4)
d_{rec}	12	-	-	days	Days required for recovery of mild cases (10)
f_{hos}	-	-	-	-	$f_{hos} = CFR_{hos} - i(t)f_{icu}$
f_{icu}	0.3 (0.31)	0.02 (0.02)	-	-	CFR of ICU patients (estimated from data fit Fig. 4)
h	0.015	0.005	-	-	Fraction of hospitalized cases (estimated from under registration and Sanquin studies (16))
$i(t)$	0.18-1	-	-	-	Fraction of hospitalized patients in need for IC treatment (fitted on reported rates from hospitalization and ICU with Gaussian smoothing conform Fig. 4)
$CFR_{hos} = \frac{f_{hos}}{f_{hos} + i(t)f_{icu}}$	0.3	-	-	-	Aggregated CFR of hospitalized and ICU cases (estimated from reported mortality rates until 7 April 2020)

434

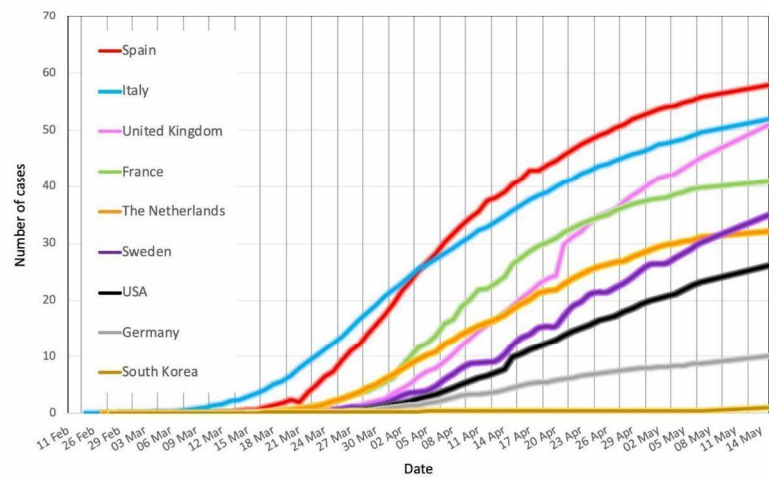
medRxiv preprint doi: <https://doi.org/10.1101/2020.05.16.20102947>; this version posted May 20, 2020. The copyright holder for this preprint (which was not certified by peer review) is the author/funder, who has granted medRxiv a license to display the preprint in perpetuity. It is made available under a CC-BY-ND 4.0 International license.

435 **LEGEND TABLE 1**

436 **Parameters for the SEIR model.** The mean and standard deviation of prior and posterior (in
437 parentheses) normal distributions of the model parameters. For each ensemble member, the
438 patient (treatment) times d_{hos} , d_{hosrec} , d_{hosdr} , d_{icarec} and d_{icud} are represented with a Gamma
439 distribution with mean sampled from $N(E_{mean}, E_{stddev})$ and standard deviation of G_{stddev} .

medRxiv preprint doi: <https://doi.org/10.1101/2020.05.16.20102947>; this version posted May 20, 2020. The copyright holder for this preprint (which was not certified by peer review) is the author/funder, who has granted medRxiv a license to display the preprint in perpetuity. It is made available under a CC-BY-ND 4.0 International license.

440 FIGURE 1



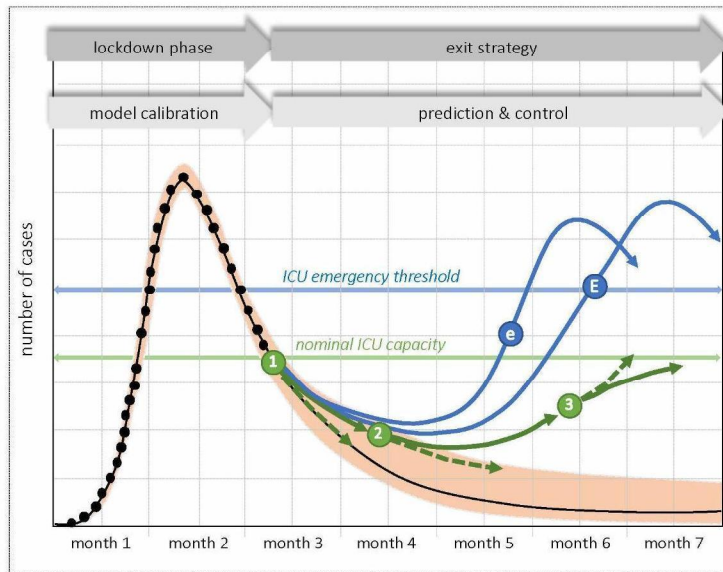
441

medRxiv preprint doi: <https://doi.org/10.1101/2020.05.16.20102947>; this version posted May 20, 2020. The copyright holder for this preprint (which was not certified by peer review) is the author/funder, who has granted medRxiv a license to display the preprint in perpetuity. It is made available under a [CC-BY-ND 4.0 International license](#).

442 **LEGEND FIGURE 1**

443 **COVID-19 mortality per 100,000 population per country (2)** The Netherlands rank
444 intermediate (orange line) between Spain / Italy (high mortality) and Germany / South Korea
445 (low mortality).

446 FIGURE 2

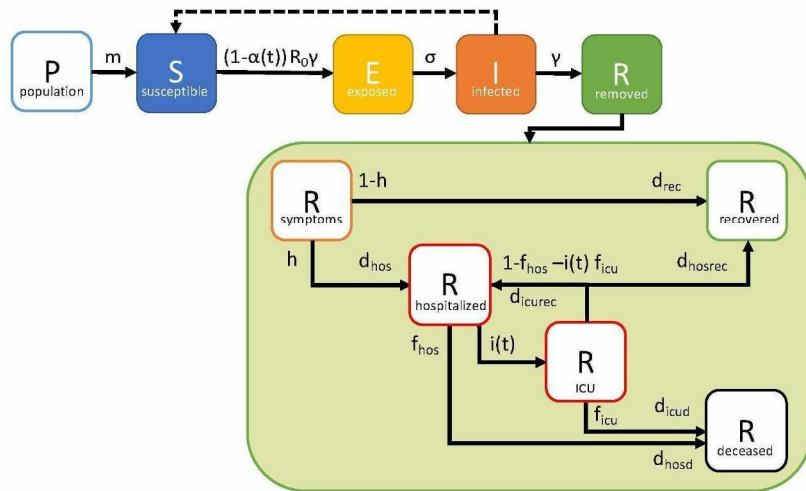


447

448 **LEGEND FIGURE 2**

449 **Schematic diagram of ICU needs, rapidly growing during the initial outbreak and**
450 **subsequently deflected under lockdown and social distancing conditions.** The exit strategy
451 is aimed at a tradeoff between limited spreading and maximizing relaxation of social
452 distancing. Two exit strategies have been considered: a progressive relaxation (blue arrows),
453 and alternatively the adaptive COVID-19 cruise control (ACCC-green arrows). In the
454 progressive scenario, an emergency brake is activated if ICU needs grow beyond the ICU
455 emergency threshold level (**E**), or if the daily ICU growth rate exceeds a threshold level (**e**).
456 The ACCC incorporates a biweekly adjustment of social distancing measures to flatten toward
457 a targeted nominal ICU capacity. Relaxed social distancing steps are taken at evaluation toll
458 gates **(1)** and **(2)**. The relaxing measures need to be adjusted in time to constraining measures
459 to avoid unsolicited growth above nominal ICU capacity. To this end, restrictive measures are
460 taken at toll gate **(3)**. For the ACCC, the dashed and solid arrows denote the default and
461 adjusted ICU trends due to the measures at the tollgates.

462 FIGURE 3

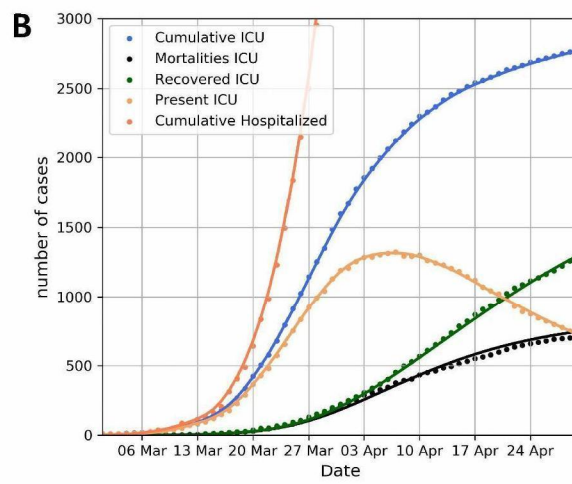
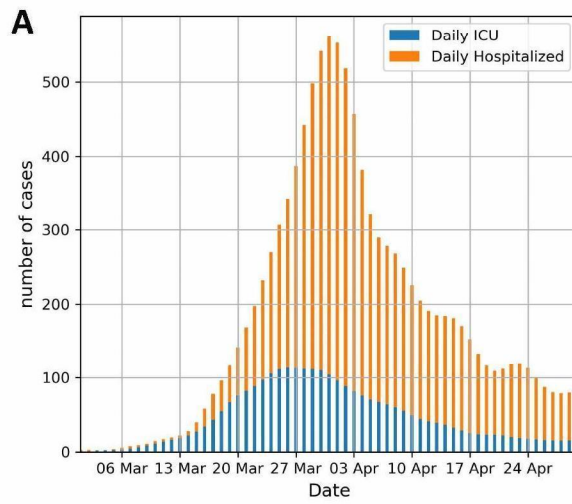


463

464 **LEGEND FIGURE 3**

465 **Schematic diagram of the SEIR model, extended for R with sub-compartments for the flow**
466 **of hospitalized patients (fraction h), and subsequently ICU patients (fraction $i(t)$).** The
467 recovery time from mild symptoms, delay and treatment times for hospitalization, and ICU
468 are marked by d_{hos} , d_{rec} , d_{hosrec} and d_{icurec} , respectively. The CFR and associated treatment periods
469 for hospitalized and ICU fatal patients are marked by f_{hos} , d_{hosd} and f_{icu} , d_{icudr} , respectively.
470 Recovered ICU patients first flow back to hospital and are assumed to take d_{hosrec} for full
471 recovery. Each of the parameters can be marked by a priori constants or distributions, which
472 can be adjusted in the data calibration. Table 1 lists the adopted parameter values including
473 the prior and posterior parameters used for the case study of the Netherlands. Some of the
474 treatment times are marked by a logistic spread represented by a Gamma distribution (see
475 Table 1).

476 FIGURE 4



477

478 **LEGEND FIGURE 4**

479 **The Netherlands' COVID-19 ICU characteristics (period of March and April 2020). (A)**

480 Daily in-hospital and ICU admissions adjusted with a Gaussian smoother with a standard
481 deviation of 1.5 days. **(B)** Cumulative counts of hospitalized and ICU admissions (actual data

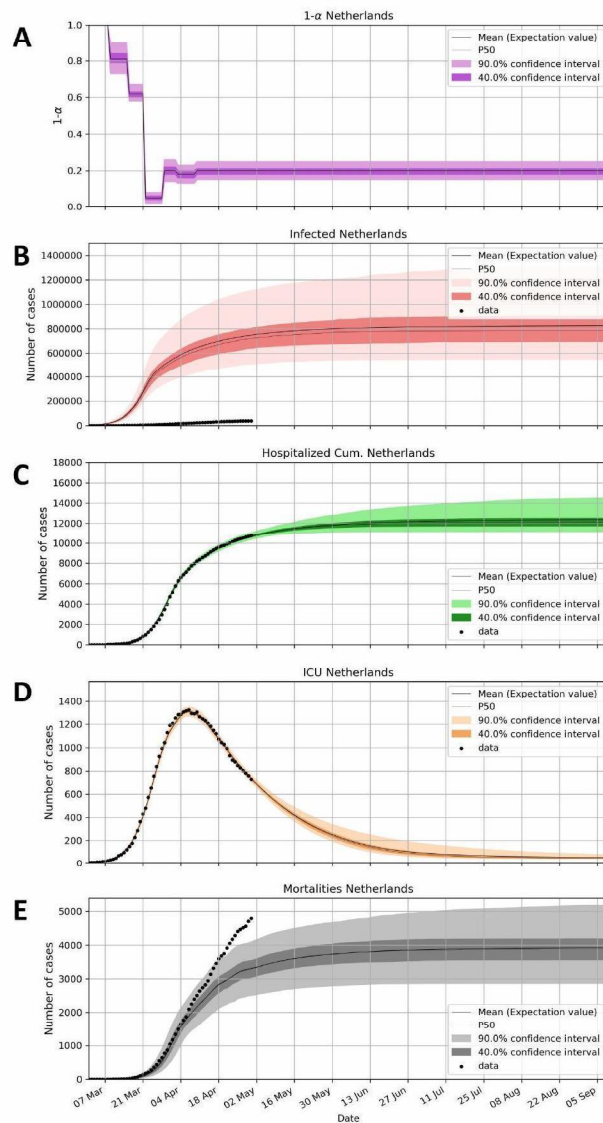
482 and smoothed lines). The daily ICU occupancy, cumulative recoveries and mortality (14) have

483 been forecasted from the daily ICU admission data with Gamma distributions for ICU

484 treatment times which differ for mortality and recovery (see Table 1). The estimated ICU

485 mortality rate is 30%.

486 FIGURE 5



487

488 **LEGEND FIGURE 5**

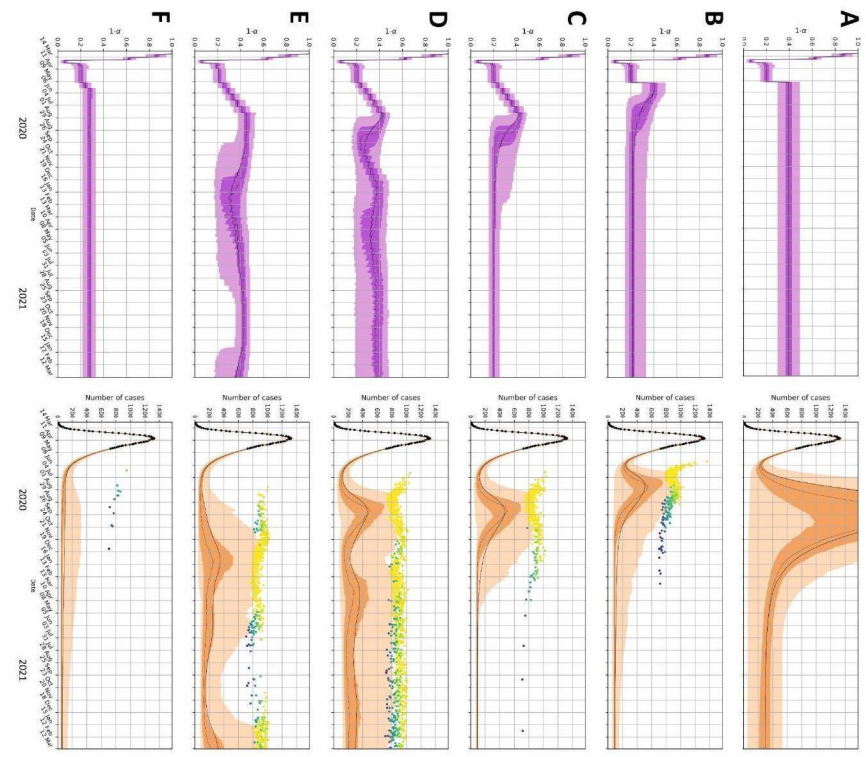
489 **Calibrated ensemble forecast based on the Netherlands' data up until the end of April 2020.**

490 **(A)** relative strength of transmission, due to social distancing measures, relative to the start

491 **(1.0)** of the outbreak, **(B)** cumulative infected people, **(C)** cumulative hospitalized, **(D)** ICU

492 occupancy, and **(E)** mortality. See text for explanation.

493 FIGURE 6

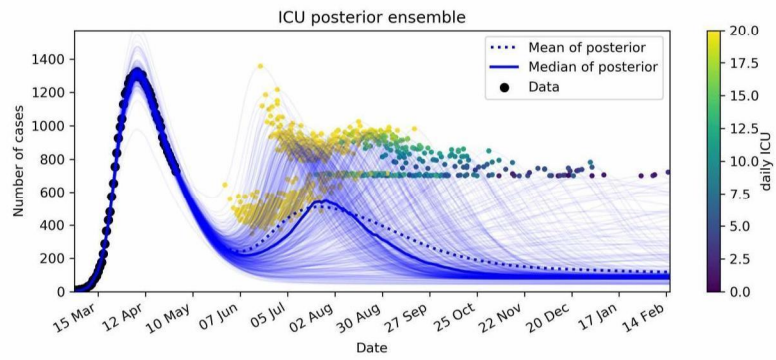


494

495 **LEGEND FIGURE 6**

496 **Progressively relaxing exit strategy.** (A) Large step-change with no emergency brake. (B)
497 Same as panel A but with emergency brake (C) Small step-changes with emergency brake.
498 (D) same as panel C with restart of relaxation when ICU < 500. (E) same as panel D with
499 marked by seasonal fluctuation of R_{eff} with a cosine function ranging from R_{eff} ~3.4 on 1 March
500 2020 to R_{eff} ~2.4 on 1 September 2020. (F) same as panel C with two progressively relaxing steps.
501 Figure conventions same as Fig. 3. The dots in the right-hand panels depict the height and
502 time of the peak ICU reached after each instance the emergency brake was activated in the
503 ensemble members. The color of the dots corresponds to the daily ICU growth at the time of
504 triggering the emergency brake (see Fig. 7).

505 FIGURE 7

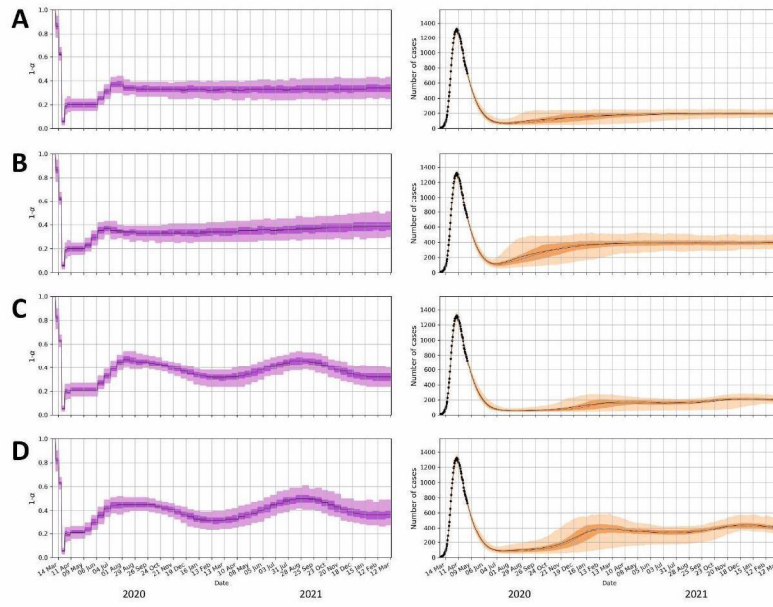


506

507 **LEGEND FIGURE 7**

508 **Emergency Brake.** Ensemble members (500) for the scenario shown in **Fig. 6B**. Two dots are
509 shown for each member of the ensemble: one at the day and ICU level the emergency brake
510 is triggered and one at the day the peak ICU is reached. The dots are colored according the
511 daily ICU growth rate at the moment of triggering of the emergency brake. Yellow dots
512 represent activation of the emergency brake by daily ICU growth rate >20 . Others have been
513 triggered by ICU >700 .

514 FIGURE 8



515

516 **LEGEND FIGURE 8**

517 **Adaptive COVID-19 cruise control (ACCC) exit strategy for two ICU nominal capacity**
518 **scenarios. (A, C) ICU capacity of 200 and (B, D) ICU capacity of 400. The panels (C) and (D)**
519 **are marked by seasonal fluctuation of R_0 , with a cosine function ranging from $R_0 \sim 3.4$ on 1**
520 **March 2020 to $R_0 \sim 2.4$ on 1 September 2020.**